

CHIH-DFT determination of the molecular structure infrared spectra, UV spectra and chemical reactivity of three antitubercular compounds: Rifampicin, Isoniazid and Pyrazinamide

Alejandra Favila · Marco Gallo ·
Daniel Glossman-Mitnik

Received: 4 September 2006 / Accepted: 2 January 2007 / Published online: 27 January 2007
© Springer-Verlag 2007

Abstract Three of the most frequent antitubercular agents employed against *Mycobacterium tuberculosis* are: Rifampicin, Isoniazid and Pyrazinamide. It has been proven that the use of these antitubercular agents together, shortens the treatment period from 12–18 months to 6 months [1]. In this work we use a new Density Functional Theory chemistry model called CHIH-DFT (Chihuahua-Heterocycles-Density Functional Theory) that reflects the mixture of Hartree Fock exchange and DFT exchange, according to a mixing parameter based on empirical rules suited for heterocyclic systems. This new chemistry model was used to calculate the molecular structure of these antitubercular compounds, as well as their infrared, UV spectra, chemical reactivity and electronic properties. The UV and infrared spectra were obtained by experimental techniques. The calculated molecular structure, UV and IR spectra values from CHIH-DFT were compared with experimentally obtained values and theoretical studies. These results are in good agreement with experimental and theoretical studies. We also predicted using the relative electrophilicity and relative nucleophilicity concepts as defined by Roy et al. [2] the chemical active sites for the three antitubercular compounds as well as their electronegativity, ionization potential, electron affinity, hardness, dipole moment, E_{HOMO} - E_{LUMO} gap energy, etc.

Keywords Chemical active sites · DFT · IR spectra · Isoniazid · Molecular structure · Pyrazinamide · Rifampicin · UV spectra

Introduction

Tuberculosis is an important pathology that stills takes 2 million lives every year. There are approximately 8 million people infected worldwide. In addition newly emergent drug resistant strains of *Mycobacterium tuberculosis* cause mortality in 70–90% of AIDS-stricken patients that develop tuberculosis [3]. The World Health Organization reported that more people died from tuberculosis in 1995 than in previous years [4].

In Mexico the Official Health Organization reported 127 cases of people infected with tuberculosis the first two weeks of 2006 [5].

Mycobacterium tuberculosis pertains to level 3 in the classification of dangerous infectious diseases.

Today most patients can cure from Tuberculosis using effective chemotherapy, but unfortunately new drug resistant strains have hindered the effect of the chemotherapy. Among the mostly used agents against drug-resistant tuberculosis are: Isoniazid $C_6H_7N_3O$ (INH), Rifampicin $C_{43}H_{58}N_4O_{12}$ (RIF), and Pyrazinamide $C_5H_5N_3O$ (PZA) [6]. Agents effective against tuberculosis can be divided in broad spectrum agents and narrow spectrum agents [1].

Rifampicin belongs to the broad spectrum classification. Rifampicin is included in drug regimes for the treatment of tuberculosis, leprosy and mycobacterial infections in patients with AIDS [1]. Isoniazid and Pyrazinamide are narrow spectrum agents against tuberculosis. Isoniazid has been used since 1952 in the treatment of tuberculosis, but is ineffective against newly emergent strains of *Mycobacterium tuberculosis* [3].

Pyrazinamide apparently fights semidormant tubercle bacilli less affected by other drugs [1]. The inclusion of PZA with INH and RIF shortens the treatment period from

A. Favila · M. Gallo · D. Glossman-Mitnik (✉)
Grupo NANOCOSMO and PRINATEC, CIMAV,
S.C., Miguel de Cervantes 120, Complejo Industrial Chihuahua,
Chihuahua Chih. 31109, Mexico
e-mail: daniel.glossman@cimav.edu.mx

12 to 18 months to 6 months, and these three drugs together constitute the short therapy “DOTS” (directly observed therapy, short course) employed by the WHO (World Health Organization) [3].

The objective of this work is to perform a detailed calculation of the molecular structure of these three antitubercular agents using a new model chemistry CHIH-DFT, as well as to predict their Infrared (IR),UV spectra, chemical reactivity sites, and molecular descriptor such as: electronegativity, ionization potential, electron affinity, hardness, dipole moment, E_{HOMO} - E_{LUMO} gap energy, etc.

Theory and computation details

The computations were performed with the GAUSSIAN 03W [7] package, with density functional methods. The equilibrium geometries of the molecules were determined by the gradient technique. The force constants and vibrational frequencies were determined by the FREQ calculations on the stationary points obtained after the optimization to verify if there were true minima. The basis sets used in this work were 3-21G* and 6-31G(d,p) (for their explanation see [8]). Additionally, the CBSB2**, CBSB7, CBSB4 and CBSB1 basis sets were used. The CBSB7 has the form 6-311G(2d,d,p) and has been developed by Petersson and co-workers as a part of the Complete Basis Set CBS-QB3 energy compound method [9]. It was designed for obtaining the best results for optimization of geometries and they found that this basis set was necessary for obtaining acceptable results on the full G2 test set [10]. The CBSB2** basis set is essentially the same as 6-31G(d,p), but with the exponents for the d functions taken from the 6-311G basis set, and is also called 6-31G†† [8, 11, 12]. The CBSB4 basis set is identical to 6-31+G(d,p) on H–Si and to 6-31+G(df,p) on P, S and Cl. The CBSB1 basis set is identical to 6-31+g(d,p) on H and He, to 6-311+G(2df) on Li–Ne, and to 6-311+g(3d2f) on Na–Ar. The CBSB2**, CBSB4 and CBSB1 basis sets are also part of the CBS-QB3 method [9].

Density functionals used in this study are a modification of those incorporated in the GAUSSIAN 03W computational package [7]. In this study we have employed a CHIH-DFT model chemistry that works well with heterocyclic molecules. The implementation is a slight different version of the PBE0 hybrid density functional [13].

In the PBE0 (or PBE1PBE one-parameter) functional, there is only one coefficient which is theoretically adjusted

Fig. 1 Optimized molecular structure using with DFT-CHIH-small model. **a)** Isoniazid (INH), **b)** Pyrazinamide (PZA) and **c)** Rifampicin (RIF)

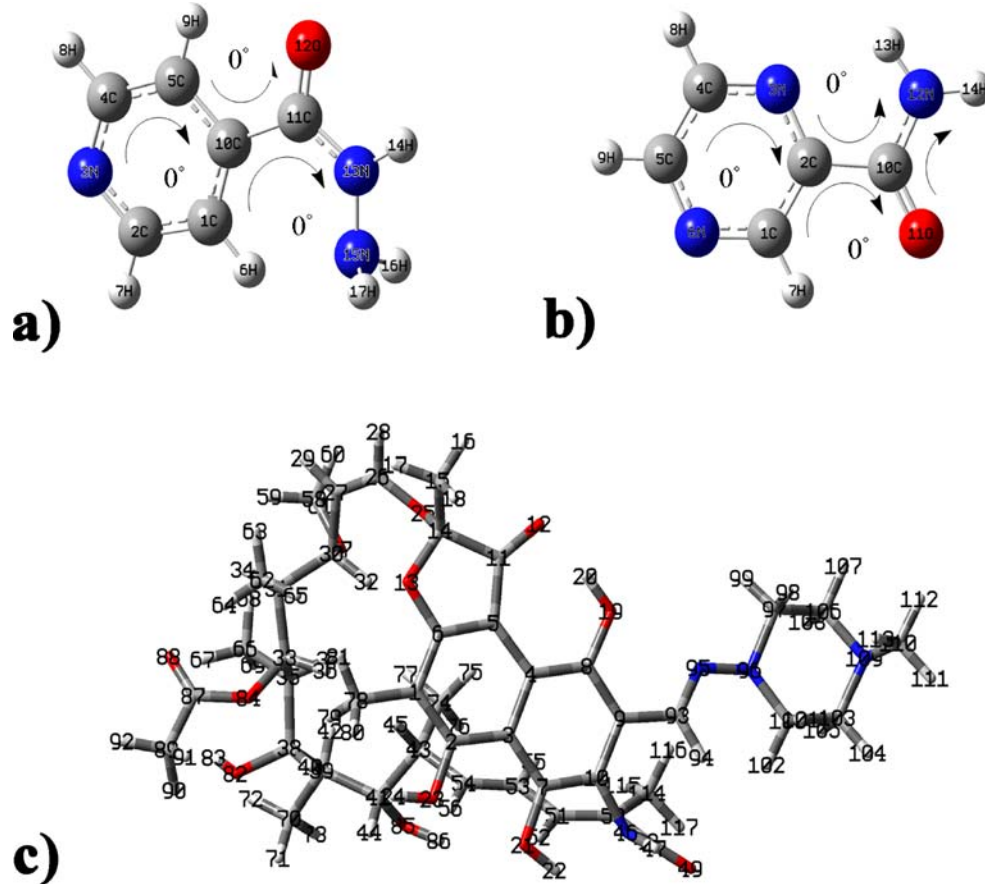


Table 1 Geometric values for the Isoniazid neutral molecule, calculated using CHIH-DFT with their three basis sets: CHIH-small-DFT, CHIH-medium-DFT and CHIH-large-DFT

Geometry of isoniazid				Exp A°
Bonds	Theoretical CHIH-s- DFT	CHIH-m- DFT	CHIH-l- DFT	
R(C1-C2)	1.397	1.397	1.397	1.394
R(C2-N3)	1.350	1.338	1.338	1.334
R(N3-C4)	1.354	1.339	1.339	1.334
R(C4-C5)	1.390	1.393	1.393	1.385
R(C5-C10)	1.400	1.400	1.400	1.403
R(C10-C1)	1.400	1.399	1.399	1.388
R(C10-C11)	1.502	1.504	1.504	1.485
R(C11-O12)	1.248	1.224	1.224	1.234
R(C11-N13)	1.374	1.376	1.376	1.332
R(N13-N15)	1.421	1.392	1.392	1.413
SD=	0.012	0.017	0.017	
Angles	Theoretical CHIH-s- DFT	CHIH-m- DFT	CHIH-l- DFT	Exp A°
A(C2-C1-C10)	118.473	118.440	118.506	119.800
A(C1-C2-N3)	124.026	124.435	124.280	123.600
A(C2-N3-C4)	116.819	116.508	116.690	116.500
A(C4-C5-C10)	119.415	119.009	119.069	119.400
A(N3-C4-C5)	123.241	123.934	123.792	124.100
A(C1-C10-C5)	118.025	117.655	117.644	116.500
A(C1-C10-C11)	128.016	126.245	126.285	125.200
A(C5-C10-C11)	113.960	115.965	115.933	118.300
A(C10-C11-O12)	120.370	120.734	120.559	122.200
A(C10-C11-N13)	121.458	120.368	120.544	115.500
A(O12-C11-N13)	118.172	118.889	118.893	122.000
A(C11-N13-N15)	126.310	124.618	124.986	120.700
SD=	3.236	2.350	2.443	

The experimental values (Exp) were obtained from [27]. The standard deviation was calculated for each theoretical model with respect to the experimental value

to 0.25, reflecting the mix of Hartree-Fock or exact exchange and the DFT exchange which is represented by the PBE density functional [14]. The correlation part is also represented by the PBE correlation functional [14] with coefficient equal to one. Our proposed density functional model, which we have called PBEg, is the same as PBE0, but with the mixing coefficient g which adopts different values depending on the number of heteroatoms in the studied molecule, or, in turn, of its molecular structure. The value of g can be calculated through the following empirical formula: $g = 0.02 + 0.14 \times \text{FHA} \times \text{FV} + 0.03 \times \text{AHA}$; where FHA is the first heteroatom chosen as the one

less electronegative, FV is valence factor which represents the oxidation state of the FHA (i.e., one for the first oxidation state, two for the second, and so on), and AHA are the number of additional heteroatoms besides the FHA. For example, for the INH compound, the g coefficient will be $g = 0.02 + 0.14 \times (1) \times (1) + 0.03 \times (0) = 0.16$, thus implying that 16% of HF exchange will be mixed with 84% of PBE exchange. For those cases in which the molecule has several heterocyclic rings, the coefficient g is calculated by averaging the coefficient for each heterocycle.

To define our model chemistry, we have to couple the proposed density functional with one or more basis sets. In this way, the new model chemistry that we have called CHIH-DFT can be represented by the expression CHIH=P-BEg/basis sets. There are three different CHIH-DFT model chemistries: CHIH(small) that uses the 3-21G* basis set for geometry optimizations and frequency calculations, and the CBSB2** basis set for the calculation of the electronic properties; CHIH(medium) that uses the CBSB2** basis set for geometry optimizations and frequency calculations and the CBSB4 basis set for the electronic properties; and CHIH(large) which uses the CBSB7 basis set for geometry optimizations and frequency calculations and the CBSB1 basis set for the electronic properties. In this way, by considering a compromise between accuracy and CPU time, the CHIH(large) will be used for small heterocyclic molecules, the CHIH(medium) for medium-sized molecules and the CHIH(small) for large heterocyclic molecules.

Our research group has previously used the CHIH-DFT method to calculate the molecular structure, chemical

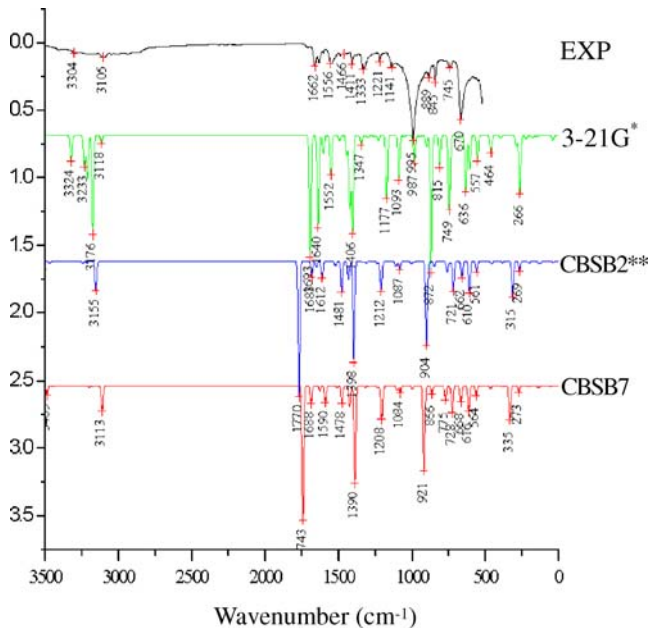


Fig. 2 Infrared spectra for Isoniazid. This figure shows the calculated IR using the three levels of theory CHIH-small-DFT (green), CHIH-medium-DFT (blue), CHIH-large-DFT (red), and the experimental IR spectra (black)

Table 2 Principal peaks of the Isoniazid experimental and calculated infrared spectra, calculated using CHIH-DFT, along with their corresponding vibrations

Theoretical calculations			Experimental	Vibrations
CHIH-small cm^{-1}	CHIH-me cm^{-1}	CHIH-large cm^{-1}	cm^{-1}	
3324	3433	3418	3304	Asym. Stretching NH2
3233	3353	3346	3105	Sym. Stretching NH2
1693	1714	1699	1662	Stretching C11O12
1640–1552	1644–1479	1637–1593	1466–1411	Ring stretching, In-plane bending C-H, Wagging NH2
1177–464	723	855–728	1141–670	Out-of-plane C-H

reactivity, UV, and IR spectra of diverse compounds such as: megazol, azathiophenes, soladinine and organic corrosion inhibitors and flavonoids. The excellent agreement of our calculations using CHIH-DFT with experimental studies is noticed [15–23].

The calculation of the ultraviolet spectrum (UV-vis) has been performed by solving the time dependent Kohn-Sham equations according to the method implemented in GAUSSIAN 03W [24–27]. The equations have been solved for 10 excited states. The ZINDO/S method was also used for calculation of the UV-vis spectra [28–32]. The IR and ultraviolet (UV-vis) spectra were calculated and visualized using the SWizard program [33].

The chemical active sites for nucleophilic, electrophilic and radical attack for each antitubercular compound were

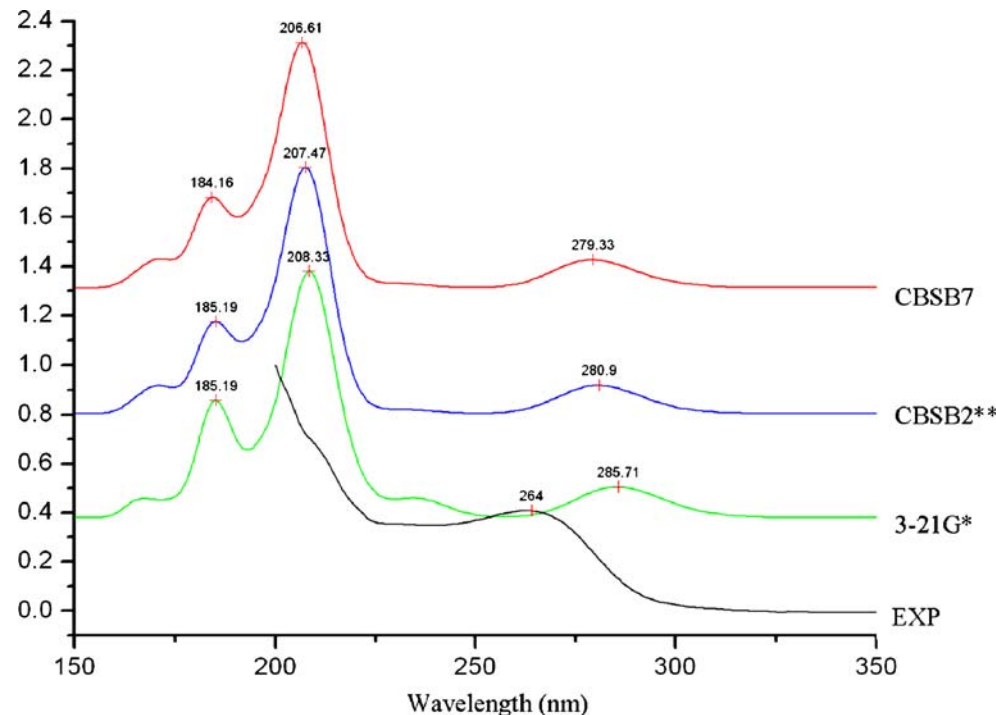
calculated using the methodology of Roy et al. [2], that defines the nucleophilic attack as the highest value of the (f_k^+ / f_k^-) ratio of the positive and negative condensed Fukui functions [34], and for electrophilic attack the highest value of the (f_k^- / f_k^+) ratio. For the radical attack we take average of $(f_k^- / f_k^+ + f_k^+ / f_k^-) / 2$. The condensed Fukui functions are found by taking the finite difference of the population analysis of the charges, depending on the direction of the electron transfer. We employ the Hirshfeld method to calculate the atomic charges [35]. The Hirshfeld has been proven to produce nonnegative fukui indices [2].

$$f_k^+ = q_k(N+1) - q_k(N)$$

$$f_k^- = q_k(N) - q_k(N-1)$$

where q_k is the gross charge of atom k in the molecule.

Fig. 3 Experimental and calculated UV spectra for Isoniazid. The theoretical spectra was calculated using ZINDO/S based on the optimized geometries obtained by CHIH-small-DFT (green), CHIH-medium-DFT (blue) y CHIH-large-DFT (red) calculated in gas, and Experimental (black) obtained in water



Experimental techniques

For the calculation of the IR spectra we used a Perkin Elmer Spectrum GX, and for obtaining the UV spectra we employed a Perkin Elmer UV-vis, Lambda 10, with a 1 cm quartz cell.

Results and discussion

Isoniazid

Figure 1 incise a) shows the representation of the optimized molecular structure using CHIH-small-DFT along with atoms labeling and numbering for Isoniazid. This molecule is planar, with the exception of the NH_2 group, located slightly out of the plane.

The results of the equilibrium conformation of the neutral molecule of Isoniazid calculated by CHIH (large); CHIH (medium) and CHIH (small) along with the experimental X-ray crystallographic structure [36] are shown in Table 1.

The standard deviation of the interatomic bond distances from their experimental values is in the range 0.012–0.017, and the standard deviation for the interatomic bond angles from their experimental values is in the range 2.35–3.23. Establishing a compromise between low standard deviations from experimental values in the interatomic bond distances and bond angles, the CHIH-medium-DFT is the best theoretical model to represent the correct geometry for Isoniazid.

The experimental and calculated infrared spectra for the Isoniazid molecule are shown on Fig. 2. The principal peaks are displayed on Table 2. The theoretical values presented on Table 2 are not scaled. From Table 2 we can see that the best representation of the IR spectra is obtained with the CHIH-small-DFT level of theory.

The experimental IR spectra for Isoniazid agrees with those published on the literature [37, 38].

The experimental and calculated UV-vis Spectra for the Isoniazid molecule are shown on Fig. 3. The experimental UV spectra for Isoniazid agrees with those published in the literature [39]. Table 3 displays the wavelength (nm) of the peaks, excitation orbitals involved and excitation energies for the experimental and calculated (theoretical) UV spectra of Isoniazid, Pyrazinamide, and Rifampicin.

According to the ratio of the Fukui indices, the site for nucleophilic attack in Isoniazid is C10, and for electrophilic and radical attack is N15 (see Fig. 4). In Table 4 we present the results of several molecular descriptors for the three antitubercular compounds, such as: dipole moment, electron affinity, ionization potential, global hardness, HOMO and LUMO energies, electronegativity and solvation energy. The different values of the electron affinity and Ionization

potential are due to two different ways of calculating these properties. One way based on the difference of total electronic energies when adding or removing electrons in relation to the neutral molecule (called energy vertical), and

Table 3 Wavelength (nm) of the peaks, excitation orbitals, excitation energies for the experimental and calculated (Theoretical) UV spectra of Isoniazid, Pyrazinamide and Rifampicin

	Energy (eV)	UV (nm)	Orbital
Pyrazinamide:			
Experimental peaks		209	
CHIH-s-ZINDO	4.20	294.99	H-L
	5.21	238.1	H-L+1
	5.91	209.7	H-1-L
	6.57	188.6	H-4-L
	7.11	174.5	H-2-L+2
	7.73	160.4	H-3+2
	4.25	291.8	H-L
CHIH-m-ZINDO	5.20	238.9	H-L+1
	6.02	205.9	H-3-L
	6.76	183.3	H-5-L+1
	7.24	171.3	H-4-L+1
	4.28	289.8	H-L
	5.23	237.3	H-L+1
	6.04	205.3	H-3-L
CHIH-l-ZINDO	6.73	184.1	H-5-L+1
	7.25	170.9	H-4-L+1
Isoniazid:			
Experimental peaks		264	
CHIH-s-ZINDO	4.35	284.9	H-L
	5.95	208.5	H-L+1
	6.70	185.0	H-L+2
	4.43	280.1	H-L
	5.97	207.6	H-L+1
	6.72	184.2	H-L+2
	4.45	278.7	H-L
CHIH-m-ZINDO	6.00	206.8	H-L+1
	6.75	183.7	H-L+2
Rifampicin:			
Experimental peaks		473	
CHIH-s-ZINDO		333	
		255	
		236	
	2.73	453.7	H-L
	3.66	338.6	H-L+1
CHIH-m-ZINDO	3.98	311.3	H-L+3
	4.89	253.3	H-L+8
	2.85	435.3	H-L
	3.63	341.7	H-1-L
	3.84	322.9	H-L+1
	4.11	301.7	H-L+3
	4.98	249.1	H-L+8
CHIH-l-ZINDO	2.88	430.7	H-L
	3.66	338.4	H-1-L
	4.13	300.1	H-L+3
	4.87	254.8	H-L+5

Fig. 4 Charge distribution of the HOMO and LUMO orbitals for optimized Isoniazid using CHIH-medium. **a)** HOMO orbital of Isoniazid in gas, **b)** LUMO orbital of Isoniazid in gas, **c)** HOMO orbital of Isoniazid in water, **d)** LUMO orbital for Isoniazid in water, **e)** Schematic representation of Isoniazid using the tube form

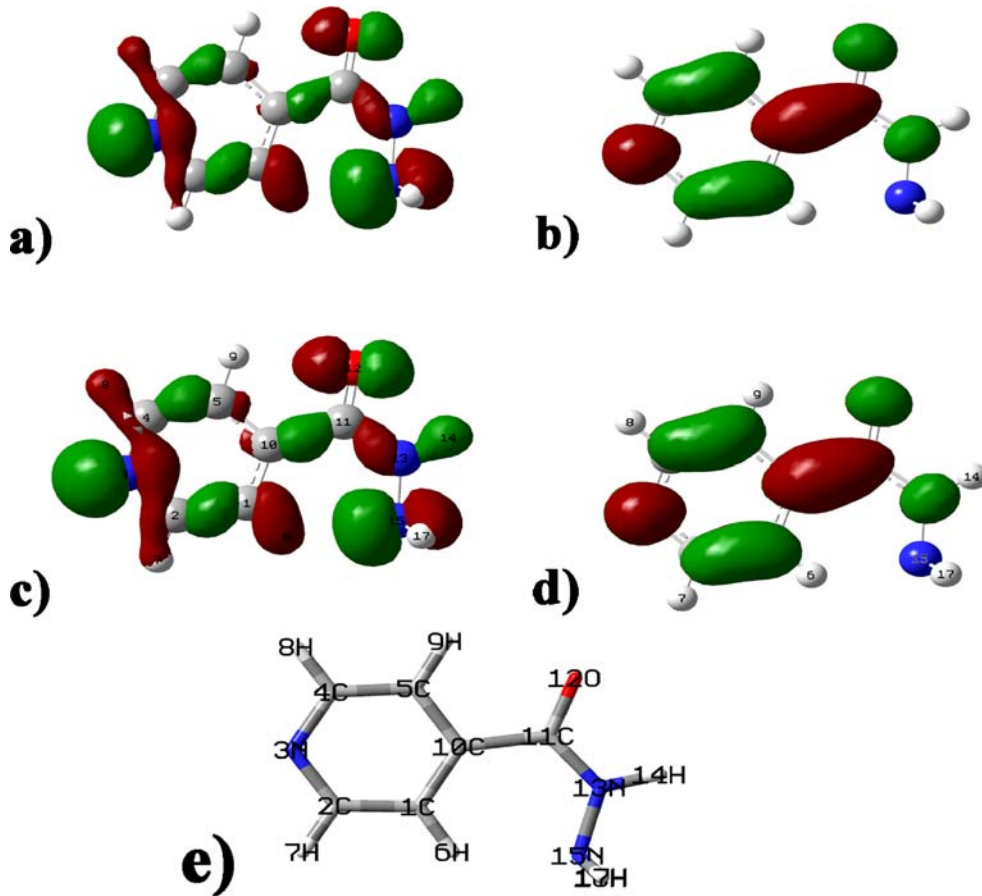


Table 4 Molecular descriptors calculated for the three antitubercular compounds

Molecular descriptor	Isoniazid		Pyrazinamide		Rifampicin	
	Gas	Solvent	Gas	Solvent	Gas	Solvent
Electon affinity						
$A = [E(0) - E(-1)]$	E	-0.5159346	1.64656575	-0.0513755	2.07349399	1.06610695
$A = [-ELUMO]$	O	1.61718539	1.70834425	2.108899	2.05502003	2.35679668
Ionization Potential eV						
$I = [E(+1) - E(0)]$	E	8.69547222	6.75057209	8.90151574	6.85055023	5.98961058
$I = [-EHOMO]$	O	6.49051083	6.61650054	6.69350937	6.78330765	4.67277595
Global Hardness ev						
$\eta = (I-A)/2$	E	4.60570344	2.55200317	4.47644562	2.38852812	2.46175182
	O	2.43666272	2.45407815	2.29230518	2.36414381	1.15798964
Electronegativity e.V.						
$X = (I+A)/2$	E	4.08976878	4.19856892	4.42507012	4.46202211	3.52785877
	O	4.05384811	4.16242239	4.40120418	4.41916384	3.51478631
Electrophilicity eV						
$\omega = \mu^2/2\eta$	E	1.78405804	3.21976177	1.8355729	3.44012791	3.33780286
	O	3.37217054	3.34823985	3.58453242	3.47561016	7.09578219
Dipole moment μ (Debyes)						
		5.2578	7.4447	3.9211	5.4505	4.5265
Solvation Energy kcal mol⁻¹						
			-10.19		-6.13	18.35
HOMO energy eV		-6.4915	-6.6165005	-6.6935093	-6.7833076	-4.67277595
LUMO energy eV		-1.6171	-1.7083442	-2.108899	-2.0550200	-2.35679668
						-1.4686100

E, energetic consideration; O, orbital consideration

Table 5 Geometric Values for the Pyrazinamide neutral molecule, calculated using CHIH-DFT with their three basis sets: CHIH-small-DFT, CHIH-medium-DFT and CHIH-large-DFT

GEOMETRY OF PYRAZINAMIDE				
	Theoretical			Exp A°
Bonds	CHIH-s-DFT	CHIH-m-DFT	CHIH-l-DFT	
R(C1-C2)	1.392	1.377	1.396	1.383
R(C1-N6)	1.349	1.309	1.332	1.329
R(C2-N3)	1.347	1.309	1.335	1.344
R(N3-C4)	1.351	1.307	1.331	1.354
R(C4-C5)	1.394	1.377	1.393	1.375
R(C5-N6)	1.354	1.308	1.334	1.353
R(C10-O11)	1.243	1.192	1.219	1.241
R(C10-N12)	1.353	1.328	1.350	1.309
SD=	0.015	0.025	0.023	
Angles	Theoretical			Exp A°
	CHIH-s-DFT	CHIH-m-DFT	CHIH-l-DFT	
A(C2-C1-N6)	121.490	121.383	121.849	122.600
A(C1-C2-N3)	122.024	121.902	121.816	121.900
A(C1-C2-C10)	118.768	119.308	119.532	120.900
A(C3-C2-C10)	119.208	118.791	118.651	117.200
A(C2-N3-C4)	116.820	116.771	116.414	115.400
A(N3-C4-C5)	121.155	121.274	121.575	122.400
A(C4-C5-N6)	122.046	122.075	122.264	121.400
A(C1-N6-C5)	116.466	116.596	116.083	116.000
A(C2-C10-O11)	121.195	120.770	121.210	119.100
A(C2-C10-N12)	112.112	114.163	113.538	117.500
A(O11-C10-N12)	126.693	125.067	125.253	123.200
SD=	2.442	1.670	1.770	

The experimental values (Exp) were obtained from [35, 36]. The standard deviation was calculated for each theoretical model with respect to the experimental value

the other way based on the HOMO and LUMO energies according to Koopman's theorem (named orbital vertical). The chemical hardness is a measure of the resistance to charge transference [40], while the electronegativity is a measure of the tendency to attract electrons in a chemical bond. The dipole moment is a measure of the charge density in the molecule [19]. Based on the molecular descriptors on Table 3. Isoniazid has a high ionization potential and a high global hardness, which means high stability and low reactivity, also it is a very polar molecule based on a high dipole moment, and it has a low electron affinity, which means that it does not take electron easily. The solvation energy of Isoniazid ($-10.19 \text{ kcal mol}^{-1}$) is the largest of the three antitubercular compound, which correlates with experimental findings that shows that Isoniazid has the highest solubility in water of the three antitubercular compounds studied [41].

Pyrazinamide

Figure 1 incise b) shows the representation of the optimized molecular structure using CHIH-small-DFT along with atoms labeling and numbering for Pyrazinamide. This molecule is planar.

The results of the equilibrium conformation of the neutral molecule of Pyrazinamide calculated by CHIH

(large); CHIH (medium) and CHIH (small) along with the experimental X-ray crystallographic structure [42, 43] are shown in Table 5. The standard deviation of the interatomic

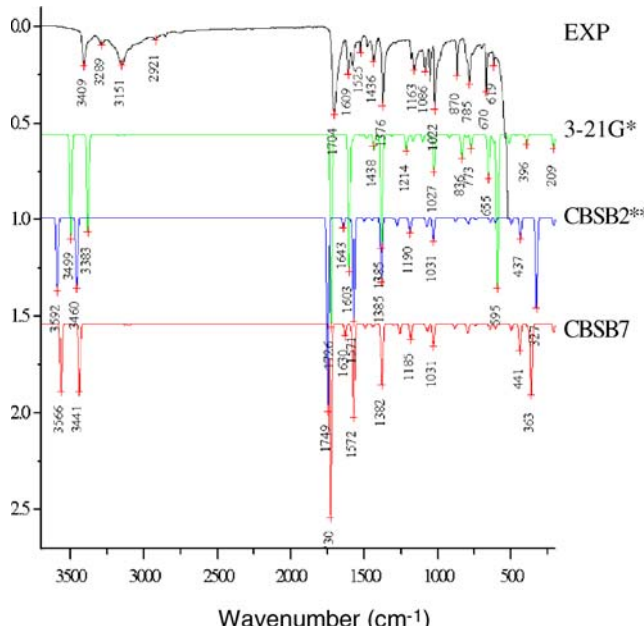


Fig. 5 Infrared spectra for Pyrazinamide. This figure shows the calculated IR using the three levels of theory CHIH-small-DFT (green), CHIH-medium-DFT (blue), CHIH-large-DFT (red), and the experimental IR spectra (black)

Table 6 Principal peaks of the Pyrazinamide, experimental and calculated Infrared spectra, calculated using CHIH-DFT, along with their corresponding vibrations

Theoretical			Experimental Vibrations	
CHIH-s cm ⁻¹	CHIH- m cm ⁻¹	CHIH- l cm ⁻¹	cm ⁻¹	
3499	3592	3566	3409	Asym. Stretching NH2
3383	3460	3441	3289	Sym. Stretching NH2
1726	1749	1730	1704	Stretching C11O12, C10N12. Out-of-plane bend N12H14
1603	1643– 1571	1630– 1572	1609	Scissoring NH2
1438– 1385	1385	1382	1525–1436	In-plane-bending C1H7, C4H8, C5H9, N12H14. Stretching N12C10
1214– 1027	1190– 1031	1185– 1031	1163–1022	Ring stretching. In plane blending C-H.

bond distances from their experimental values is in the range 0.015–0.023, and the standard deviation for the interatomic bond angles from their experimental values is in the range 1.67–2.44.

The CHIH-medium-DFT is the best theoretical model to represent the correct geometry for Pyrazinamide, since it has the lowest standard deviation for both the interatomic bond distances and the bond angles.

Chis et al. [43] conducted a theoretical study of Pyrazinamide. They used the DFT B3LYP/6-31G(d) method to predict the geometry of two conformers (C1, C2) and a Pyrazinamide dimer, and for the IR spectra they used the B3LYP/6-31G(d) and BLYP/6-31G(d) methods to predict the vibrations.

Our Theoretical results agree with those from Chis et al. [43] for conformer C1. The standard deviation for the interatomic bond distances with respect to the experimental values gave them a value close to 0.023 while for the interatomic bond angles they obtain a standard deviation value of 3.09. This value for the standard deviation of the bond angles is higher than our value of 1.670 predicted with the CHIH-medium-DFT level of theory.

The experimental and calculated infrared spectra for the Pyrazinamide molecule is shown on Fig. 5. The principal peaks are displayed on Table 6. The theoretical values presented on Table 6 are not scaled. From Table 6 we can see that the best representation of the IR spectra is obtained with the CHIH-small-DFT level of theory. The values for the vibrations obtained using the CHIH-small-DFT are in agreement with those calculated by Chis et al. [43] for conformer C1 using DFT B3LYP/6-31G(d).

The experimental IR spectra for Pyrazinamide agrees with those published on the literature [38, 43, 44].

The experimental and calculated UV-vis spectra for the Pyrazinamide molecule are shown in Fig. 6. Our experimentally calculated UV spectra for Pyrazinamide shows two peaks at 209 nm, and 270 nm, while those published in the literature show two peaks at 270 nm and 320 nm [43]. Our theoretical UV spectra showed five peaks in the 171–295 nm range. Table 3 displays the wavelength (nm) of the peaks, excitation orbitals involved and excitation energies for the experimental and calculated (Theoretical) UV spectra of Pyrazinamide.

According to the ratio of the Fukui indices, the site for nucleophilic attack in Isoniazid is C2, and for electrophilic and radical attack is O11 (see Fig. 7).

Based on the molecular descriptors in Table 4 Pyrazinamide has a high ionization potential, and a high global hardness, which means high stability and low reactivity, also it is a very polar molecule based on a high dipole moment, and it has a low electron affinity, which means that it does not takes electron easily. Its solubility in water is lower than Isoniazid but higher than Rifampicin, shown by the value of the solvation energy [41].

Rifampicin

Figure 1 incise c) shows the representation of the optimized molecular structure using CHIH-small-DFT along with atoms labeling and numbering for Rifampicin.

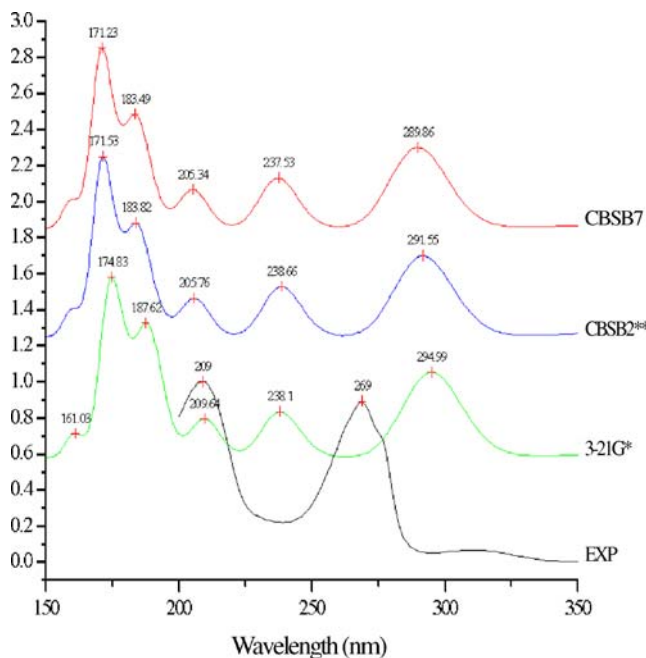


Fig. 6 Experimental and calculated UV spectra for Pyrazinamide. The theoretical spectra was calculated using ZINDO/S based on the optimized geometries obtained by CHIH-small-DFT (green), CHIH-medium-DFT (blue) y CHIH-large-DFT (red) calculated in gas, and Experimental (black) obtained in water

Fig. 7 Charge distribution of the HOMO and LUMO orbitals for optimized Pyrazinamide using CHIH-medium. **a)** HOMO orbital of Pyrazinamide in gas, **b)** LUMO orbital of Pyrazinamide in gas, **c)** HOMO Orbital of Pyrazinamide in water, **d)** LUMO orbital for Pyrazinamide in water, **e)** Schematic representation of Pyrazinamide using the tube form

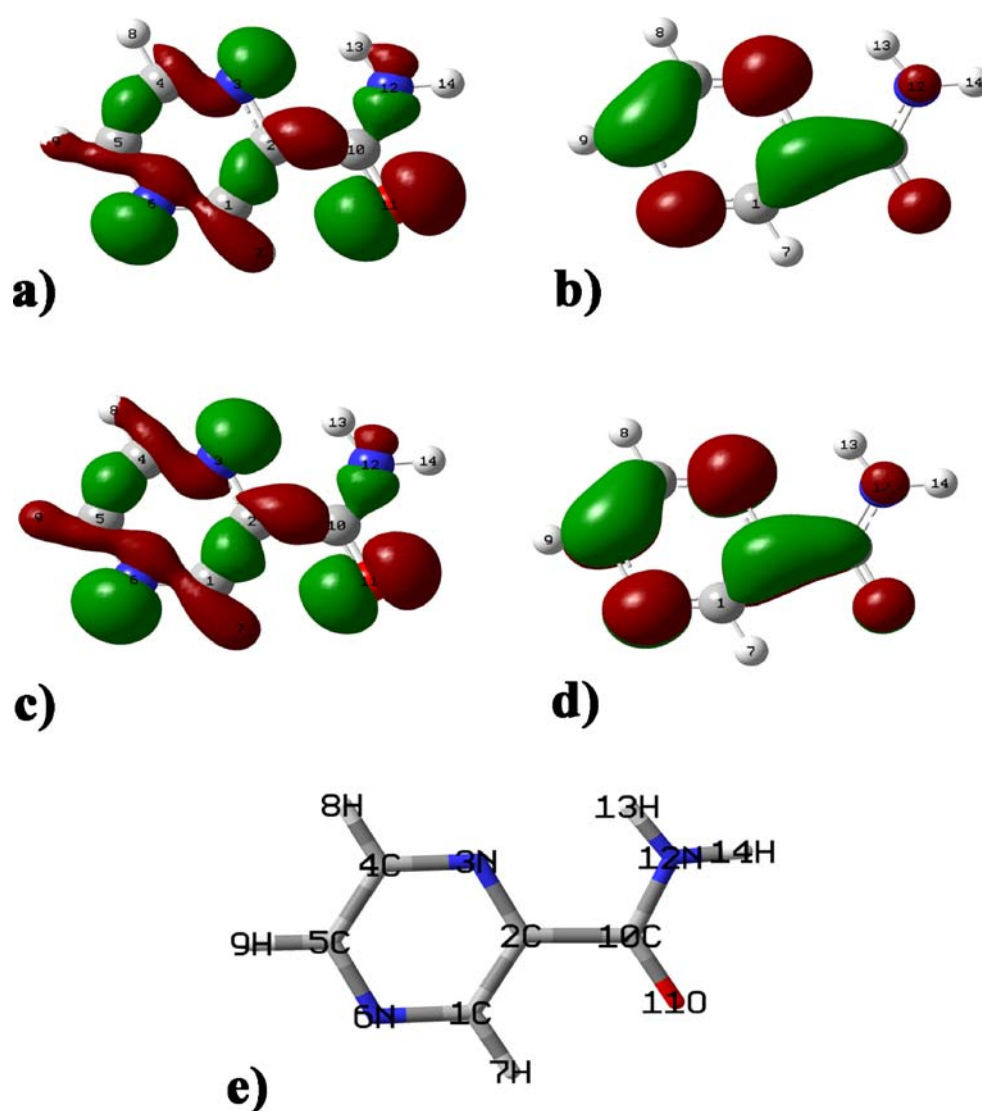


Table 7 Geometric values for the Rifampicin neutral molecule, calculated using CHIH-DFT with their three basis sets: CHIH-small-DFT, CHIH-medium-DFT and CHIH-large-DFT

Geometry of Rifampicin				
Bonds	Theoretical CHIH-s- DFT	CHIH-m- DFT	CHIH-l- DFT	Exp A°
(C1-C2)	1.399	1.400	1.3955	1.435
(C1-C6)	1.387	1.395	1.3912	1.348
(C1-C78)	1.511	1.504	1.5016	1.499
(C2-C3)	1.431	1.438	1.4351	1.474
(C2-O23)	1.364	1.343	1.3425	1.273
(C3-C4)	1.445	1.442	1.4395	1.418
(C3-C7)	1.415	1.421	1.4182	
(C4-C5)	1.440	1.444	1.4417	1.461
(C4-C8)	1.425	1.424	1.4206	1.381
(C5-C6)	1.402	1.400	1.3968	1.409
(C5-C11)	1.429	1.434	1.4325	1.393
(C6-O13)	1.390	1.358	1.3561	1.379
(C7-C10)	1.386	1.391	1.3871	1.397

Table 7 (continued)

Geometry of Rifampicin				
(C7-O21)	1.381	1.355	1.3551	1.340
(C8-C9)	1.414	1.414	1.4092	1.402
(C8-O19)	1.347	1.335	1.3353	1.374
(C9-C10)	1.410	1.417	1.4135	1.402
(C9-C93)	1.452	1.460	1.4599	1.452
(C10-N46)	1.451	1.439	1.4362	1.425
(C11-O12)	1.259	1.233	1.2298	1.260
(C11-C14)	1.546	1.545	1.5433	1.517
(O13-C14)	1.484	1.443	1.4417	1.457
(C14-C15)	1.508	1.512	1.5091	1.500
(C14-O25)	1.437	1.408	1.4078	1.414
(O25-C26)	1.413	1.373	1.3695	1.401
(C26-C27)	1.333	1.337	1.333	1.318
(C27-C30)	1.506	1.506	1.5036	1.501
(C30-C31)	1.557	1.556	1.5529	1.525
(C30-O57)	1.474	1.433	1.4344	1.457
(C31-C33)	1.546	1.549	1.5466	1.549
(C31-C62)	1.541	1.534	1.5329	1.512

Table 7 (continued)

Geometry of Rifampicin				
(C33-C35)	1.552	1.549	1.5462	1.539
(C33-O84)	1.494	1.457	1.4568	1.459
(C35-C38)	1.551	1.551	1.5492	1.537
(C35-C66)	1.540	1.533	1.5303	1.531
(C38-C39)	1.558	1.566	1.563	1.529
(C38-O82)	1.468	1.425	1.4256	1.455
(C39-C41)	1.538	1.540	1.5381	1.518
(C39-C70)	1.538	1.531	1.5296	1.537
(C41-C43)	1.562	1.558	1.5566	1.524
(C41-O85)	1.455	1.417	1.4189	1.439
(C43-C54)	1.506	1.502	1.5011	1.513
(C43-C74)	1.534	1.528	1.5272	1.545
(N46-C48)	1.432	1.412	1.4078	1.353
(C48-O49)	1.244	1.222	1.2194	1.215
(C48-C50)	1.479	1.491	1.4902	1.517
(C50-C51)	1.352	1.355	1.351	1.352
(C50-114)	1.506	1.500	1.4984	1.506
(C51-C52)	1.089	1.091	1.0892	0.922
(C51-C53)	1.448	1.448	1.446	1.460
(C53-C54)	1.352	1.352	1.3474	1.318
(O57-C58)	1.457	1.411	1.4112	1.456
(C87-O88)	1.228	1.211	1.2086	1.455
(C87-C89)	1.505	1.505	1.5024	1.455
(C93-N95)	1.307	1.297	1.2922	1.292
(N95-N96)	1.386	1.340	1.3369	1.389
(N96-C97)	1.473	1.460	1.46	1.464
(N96-C100)	1.479	1.459	1.4584	1.425
(C97-C106)	1.537	1.107	1.527	1.497
(C100-C103)	1.547	1.537	1.5359	1.497
(C103-N109)	1.473	1.099	1.4526	1.489
(C106-N109)	1.479	1.455	1.4576	1.474
(N109-C110)	1.473	1.454	1.4522	1.476
DS=	0.182	0.199	0.184	
Theoretical				
Angles	CHIH-s-DFT	CHIH-m-DFT	CHIH-l-DFT	Exp A°
(C2-C1-C6)	116.628	115.723	115.8902	116.240
(C2-C1-C78)	121.968	122.038	121.8682	119.520
(O6-C1-C78)	121.402	122.234	122.2369	124.120
(C1-C2-C3)	122.627	123.532	123.4803	119.850
(C1-C2-O23)	119.857	119.050	118.8395	120.720
(C3-C2-O23)	117.511	117.416	117.678	119.410
(C2-C3-C4)	119.815	119.350	119.2389	121.880
(C2-C3-C7)	121.535	122.084	122.129	118.820
(C4-C3-C7)	118.619	118.520	118.6012	119.240
(C3-C4-C5)	116.476	116.637	116.704	115.810
(C3-C4-C8)	120.704	120.645	120.5089	119.910
(C5-C4-C8)	122.779	122.688	122.7616	124.260
(C4-C5-C6)	120.358	120.431	120.3363	119.220
(C4-C5-C11)	132.509	133.934	133.942	133.140
(C6-C5-C11)	107.132	105.609	105.6915	107.320
(C1-C6-C5)	123.966	124.269	124.2582	126.940
(C1-C6-O13)	121.833	120.673	120.7123	121.010
(C5-C6-O13)	114.200	115.055	115.0265	112.020
(C3-C7-C10)	119.650	119.679	119.6423	119.080
(C3-C7-O21)	122.695	121.521	121.451	121.400

Table 7 (continued)

Geometry of Rifampicin				
(C10-C7-O21)	117.411	118.639	118.7102	119.470
(C4-C8-C9)	118.987	119.790	119.7777	121.590
(C4-C8-O19)	124.606	123.488	123.3515	123.140
(C9-C8-O19)	116.405	116.722	116.8688	115.270
(C8-C9-C10)	119.259	118.564	118.7218	118.450
(C8-C9-C93)	123.989	124.216	123.965	116.770
(C10-C9-C93)	116.662	117.216	117.3112	124.700
(C7-C10-C9)	122.722	122.699	122.6442	121.470
(C7-C10-N46)	115.096	115.457	115.7033	118.710
(C9-C10-N46)	121.959	121.728	121.5328	119.540
(C5-C11-O12)	132.243	132.440	132.5589	131.410
(C5-C11-C14)	107.145	106.537	106.4693	108.490
(O12-C11-C14)	120.612	121.020	120.9692	120.080
(C6-O13-C14)	106.552	107.424	107.4193	108.180
(C11-C14-O13)	104.413	104.669	104.6113	103.890
(C11-C14-C15)	113.397	113.524	113.5008	113.950
(C11-C14-O25)	103.965	104.428	104.2734	111.880
(13-C14-C15)	108.666	109.303	109.3173	109.470
(13-C14-O25)	109.282	108.398	108.2958	109.560
(C15-C14-O25)	116.391	115.813	116.0953	107.980
(C14-O25-C26)	118.625	119.399	119.6541	116.180
(O25-C26-C27)	120.912	121.870	121.8315	123.930
(C26-C27-C30)	122.145	124.150	124.376	120.390
(C27-C30-C31)	112.243	112.861	112.6339	112.750
(C27-C30-O57)	114.230	113.054	112.7011	110.080
(C31-C30-O57)	110.758	111.910	112.0142	111.090
(C30-C31-C33)	107.143	108.877	109.3504	112.990
(C30-C31-C62)	109.547	110.213	109.9398	113.270
(C33-C31-C62)	110.290	110.688	110.0776	108.940
(C31-C33-C35)	117.470	118.225	118.7713	113.500
(C31-C33-O84)	113.519	113.452	113.1808	110.070
(C35-C33-O84)	110.932	111.974	111.7545	119.370
(C33-C35-C66)	115.832	117.282	117.3065	111.450
(C38-C35-C66)	110.462	111.042	111.1857	113.960
(C35-C38-C39)	112.773	113.005	113.0293	117.980
(C35-C38-O82)	110.801	111.514	111.3737	105.490
(C39-C38-O82)	112.625	112.882	112.9875	111.120
(C38-C39-C41)	108.430	109.434	109.3902	114.140
(C38-C39-C70)	111.785	112.741	112.8161	110.460
(C41-C39-C70)	108.888	110.143	110.0204	112.630
(C39-C41-C43)	114.439	114.470	114.6989	115.600
(C39-C41-O85)	107.385	108.761	108.6284	111.260
(C43-C41-O85)	109.201	109.717	109.6133	106.340
(C41-C43-C54)	107.139	108.420	108.6	113.660
(C41-C43-C74)	110.239	112.496	112.4193	112.720
(C54-C43-C74)	113.668	108.805	113.8532	106.840
(C10-N46-C48)	119.138	122.289	123.0707	124.560
(N46-C48-O49)	120.024	119.573	119.6195	125.510
(N46-C48-C50)	115.367	117.270	117.35	114.060
(O49-C48-C50)	124.514	123.151	123.0244	120.400
(C48-C50-C51)	119.136	119.319	119.6794	124.390
(C48-C50-C114)	113.844	114.571	114.4597	112.190
(C51-C50-C114)	127.001	126.106	125.8494	122.420
(C50-C51-C53)	127.927	127.925	127.3729	129.090
(C51-C53-C54)	119.363	120.472	121.3896	122.190
(C43-C54-C53)	126.733	127.880	127.3422	127.610

Table 7 (continued)

Geometry of Rifampicin				
(C30-O57-C58)	113.723	115.856	116.009	111.090
(C33-O84-C87)	119.409	120.847	121.1293	119.370
(O84-C87-O88)	123.766	124.817	124.8535	121.920
(O84-C87-C89)	108.934	110.122	110.141	112.560
(O88-C87-C89)	127.298	125.061	125.0053	125.520
(C9-C93-N95)	124.665	123.449	122.8911	121.150
(C93-N95-N96)	117.952	120.386	121.1471	120.650
(N95-N96-C97)	112.048	112.465	112.4302	109.330
(N95-N96-C100)	123.494	122.790	122.7154	120.760
(C97-N96-C100)	116.136	115.899	116.0053	112.310
(N96-C97-C106)	109.434	110.539	110.4863	109.230
(N96-C100-C103)	108.316	109.922	109.866	111.080
(C100-C103-N109)	114.465	107.353	115.0177	110.940
(C97-C106-N109)	112.533	107.327	113.4323	111.290
(C103-N109-C106)	109.331	108.818	109.2735	109.390
(C103-N109-C110)	113.962	113.605	114.2317	117.170
(C106-N109-C110)	113.904	107.567	114.2221	112.210
DS=	3.365	3.172	3.173	

The experimental values (Exp) were obtained from [38]. The standard deviation was calculated for each theoretical model with respect to the experimental value

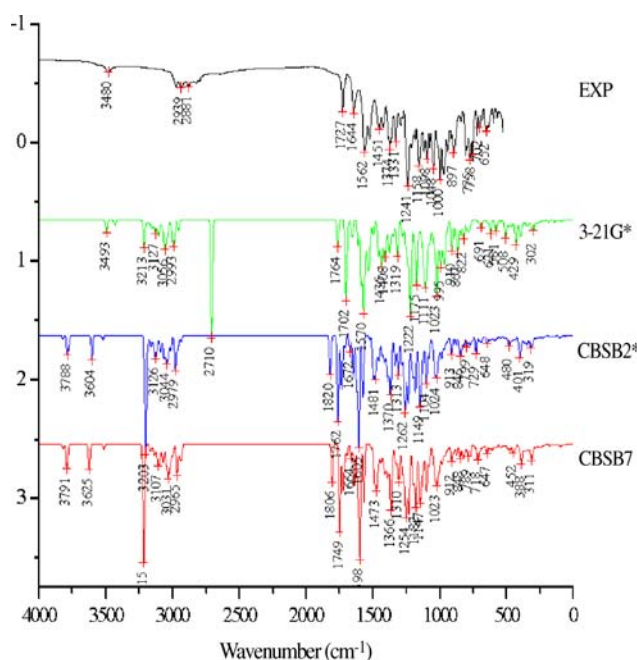


Fig. 8 Infrared spectra for Rifampicin. This figure shows the calculated IR using the three levels of theory CHIH-small-DFT (green), CHIH-medium-DFT (blue), CHIH-large-DFT (red), and the experimental IR spectra (black) taken from [39]

Table 8 Principal peaks of the Rifampicin, experimental and calculated Infrared spectra, calculated using CHIH-DFT, along with their corresponding vibrations

Theoretical	Experimental	Vibrations
3493	3788	3791
3213	3604	3625
2710	3203	2881
1702	1762	1749
1570	1672	1664
	1605	1598
867	799	789
581	729	718
508	480	452
429	401	388

This molecule is not planar at all, it has torsional angles. (e.g., $C_{100}-C_{103}-N_{109}-C_{110}=73.65$, $C_9-C_{10}-N_{46}-C_{48}=-54.81$, $C_{39}-C_{41}-C_{43}-C_{73}=-69.08$)

The results of the equilibrium conformation of the neutral molecule of Rifampicin calculated by CHIH (large); CHIH (medium) and CHIH (small) along with the experimental X-ray crystallographic structure [45] are shown in Table 7. From these results we can notice that the lowest standard deviation of the errors for the differences between the experimental and calculated bond lengths corresponds to the CHIH (small) method (0.182), and the lowest standard deviation of the errors for the

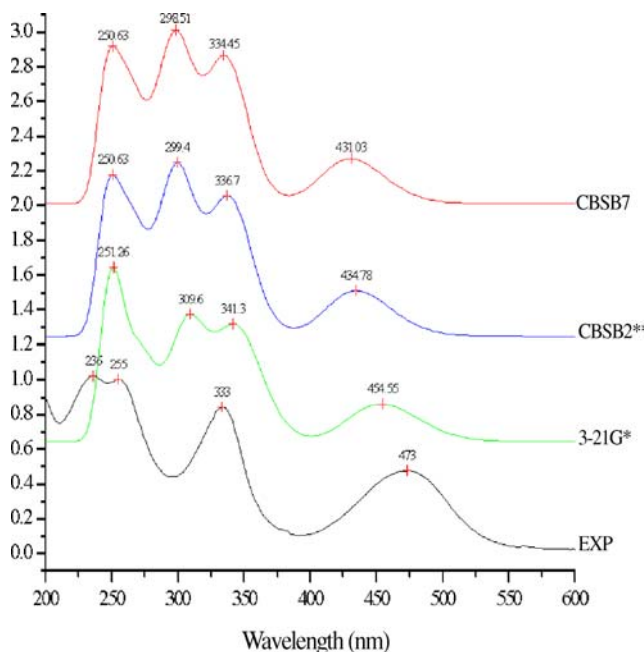


Fig. 9 Experimental and calculated UV spectra for Rifampicin. The theoretical spectra was calculated using ZINDO/S based on the optimized geometries obtained by CHIH-small-DFT (green), CHIH-medium-DFT (blue) y CHIH-large-DFT (red) calculated in gas, and experimental (black) obtained in water

differences between the experimental and bond angles corresponds to the CHIH (medium) method (3.172).

Establishing a compromise between low standard deviations from experimental values in the interatomic bond distances and bond angles, the CHIH-small-DFT is the best theoretical model to represent the correct geometry for Rifampicin.

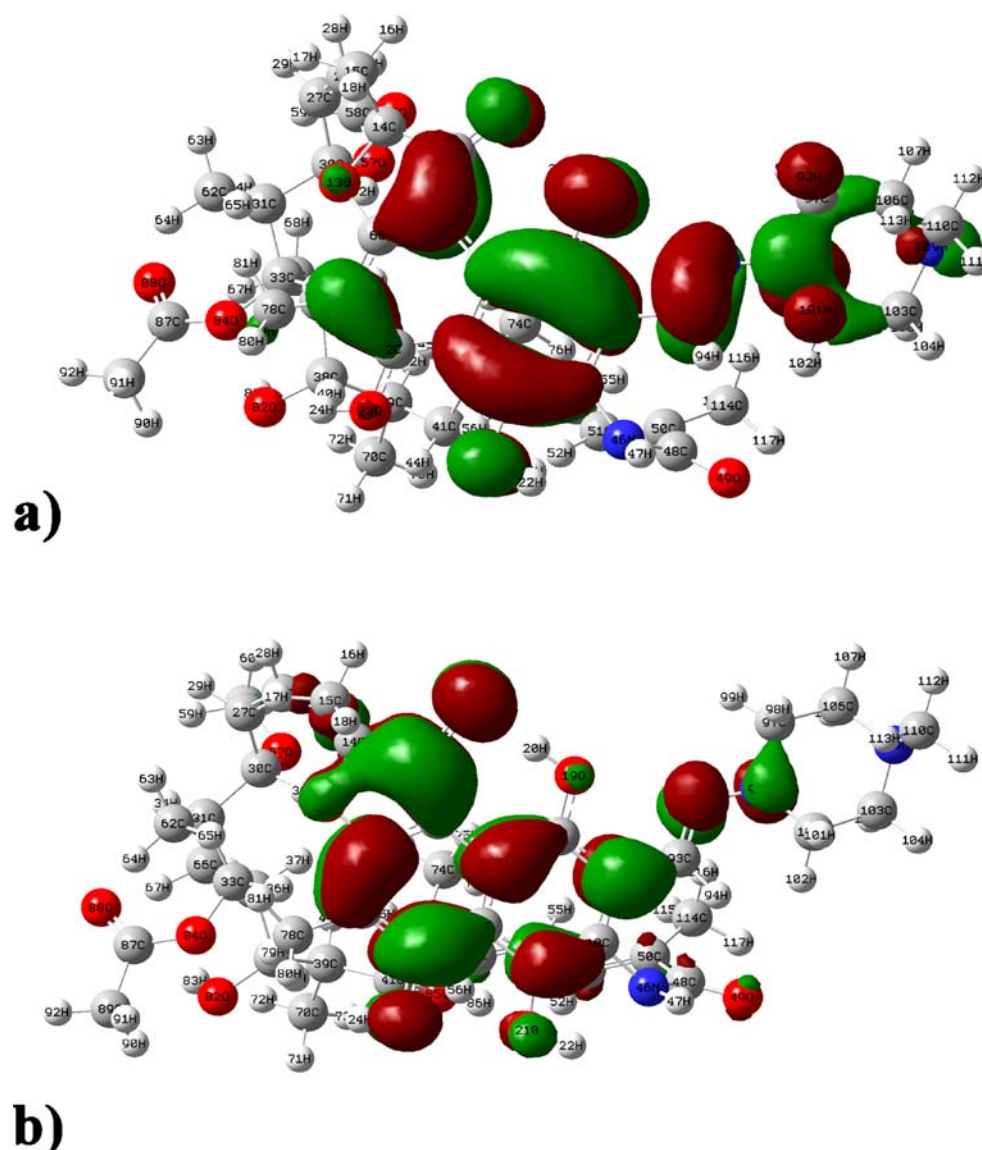
The experimental and calculated Infrared spectra for the Rifampicin molecule is shown in Fig. 8. The principal peaks are displayed on Table 8. The theoretical values presented on Table 8 are not scaled. From Table 8 we can see that the best representation of the IR spectra is obtained with the CHIH-small-DFT level of theory.

The experimental IR spectra for Rifampicin agrees with those published in the literature [46].

The experimental and calculated UV-vis spectra for the Rifampicin molecule are shown in Fig. 9. The experimental UV spectra for Rifampicin agrees with those published in the literature [47]. Table 3 displays the wavelength (nm) of the peaks, excitation orbitals involved and excitation energies for the experimental and calculated (Theoretical) UV spectra of Rifampicin.

Unfortunately due to a small number of negative fukui functions obtained in our calculations, we can not use the relative electrophilicity and nucleophilicity descriptors, defined by Roy et al. [2], to locate the chemical active sites for rifampicin. We used a new molecular descriptor $(sf)_k^\alpha$ where $\alpha = +/-0$ defined as the product of the local softness and fukui functions. This descriptor is equal to the square of the fukui function times the global softness,

Fig. 10 Charge distribution of the HOMO and LUMO orbitals for optimized Rifampicin using CHIH-medium. **a)** HOMO orbital of Rifampicin in gas, **b)** LUMO orbital of Rifampicin in GAS



which guarantees always positive values [48]. Using this molecular descriptor we obtain for Rifampicin O19>N96 as sites preferred for electrophilic attack, O12>C11 as sites preferred for nucleophilic and radical attack (see Fig. 10). Based on the molecular descriptor on Table 4, we can see that it is hard to solubilize Rifampicin in water, given by a positive value of its Gibbs energy of solvation. This poor solubility is also reflected by its low experimental solubility value [41]. Rifampicin has a higher electron affinity, and a lower ionization potential than Pyrazinamide and Isoniazid, signaling a reactivity character for this molecule.

Conclusions

The molecular structure, infrared and UV spectra for three anti-tubercular agents were calculated using the new CHIH-DFT (Chihuahua-Heterocycles-Density Functional Theory) model chemistry. Comparison with experimental data indicates that the CHIH-m-DFT method gives the best geometrical optimization of these molecules considering a compromise between computational speed and accuracy. The standard deviation between the calculated and experimental results shows that for large molecules, the CHIH-small-DFT and the CHIH-medium-DFT give better approximation and less computational time than the CHIH-large-DFT. The IR spectra calculated using the CHIH-small-DFT method gave the best agreement with experimental results. From the calculated electronic spectra of Isoniazid and Pyrazinamide we can infer that these molecules will be colorless, since the HOMO-LUMO transition takes place in the ultraviolet region. The HOMO-LUMO transition in the case of Rifampicin takes place in the visible region allowing this molecule to have color. The UV spectra at the three levels of theory CHIH-DFT, gave very similar peaks.

Calculations of the UV spectra not shown using TD-DFT do not give better results than the ZINDO/s method, and are computationally more intensive. We also predicted the chemical reactivity sites for each molecule, as well as a series of molecular descriptors such as: electronegativity, ionization potential, electron affinity, hardness, dipole moment, $E_{\text{HOMO}}-E_{\text{LUMO}}$ gap energy, and salvation energy for each molecule. Based on these molecular descriptors on Table 4, we can observe that Pyrazinamide and Isoniazid are chemical species more stable than Rifampicin. Isoniazid and Pyrazinamide can solubilize in water more easily than Rifampicin, which has a positive Gibbs energy of solvation. The importance of predicting chemical active sites can help experimentalist to better understand the mechanism of action of these antitubercular compounds.

The dipole moment is a measure of charge density in a molecule. For the three molecules analyzed the dipole

moment for Isoniazid is 5.2578 Debye, 3.9211 Debye for Pyrazinamide and 4.5265 Debye for Rifampicin.

The CHIH-DFT new model chemistry appears to be a very useful method for calculating the molecular spectra and electronic properties of heterocyclic compounds.

Acknowledgements D. Glossman-Mitnik is a CONACyT and CIMAV researcher. Alejandra Favila and Marco Gallo gratefully acknowledge doctoral and postdoctoral fellowships from the National Science and Technology Council in Mexico (CONACyT).

References

1. Chopra I, Brennan P (1998) *Tuberc Lung D* 78(2):89–98
2. Roy RK, Pal S, Hirao K (1999) *J Chem Phys* 110(17):8236–8245
3. Dessen A, Quernard A, Blanchard JS, Jacobs Jr WR, Sacchettini JC (1995) *Science* 267(1995):1638–1641
4. Manetti F, Corelli F, Biava M, Fioravanti R, Porretta GC, Botta M (2000) *Il Farmaco* 55:484–491
5. Secretaría de Salud, Mexico, Boletín epidemiología (2006) <http://www.dgepi.salud.gob.mx/boletin/2006/sem02/pdf/cua1y2.pdf>
6. Sociedad Argentina de Pediatría, Criterios de diagnóstico y tratamiento de la tuberculosis infantil (2002) *Arch Argent pediatr* 100(2):159–178
7. Frisch MJ, Trucks GW, Schlegel HB, Scuseria GE, Robb MA, Cheeseman JR, Montgomery Jr JA, Vreven T, Kudin KN, Burant JC, Millam JM, Iyengar SS, Tomasi J, Barone V, Mennucci B, Cossi M, Scalmani G, Rega N, Petersson GA, Nakatsuji H, Hada M, Ehara M, Toyota K, Fukuda R, Hasegawa J, Ishida M, Nakajima T, Honda Y, Kitao O, Nakai H, Klene M, Li X, Knox JE, Hratchian HP, Cross JB, Bakken V, Adamo C, Jaramillo J, Gomperts R, Stratmann RE, Yazyev O, Austin AJ, Cammi R, Pomelli C, Ochterski JW, Ayala PY, Morokuma K, Voth GA, Salvador P, Dannenberg JJ, Zakrzewski VG, Dapprich S, Daniels AD, Strain MC, Farkas O, Malick DK, Rabuck AD, Raghavachari K, Foresman JB, Ortiz JV, Cui Q, Baboul AG, Clifford S, Cioslowski J, Stefanov BB, Liu G, Liashenko A, Piskorz P, Komaromi I, Martin RL, Fox DJ, Keith T, Al-Laham MA, Peng CY, Nanayakkara A, Challacombe M, Gill PMW, Johnson B, Chen W, Wong MW, Gonzalez C, Pople JA (2004) Gaussian 03, Revision C.02. Gaussian, Wallingford, CT
8. Foresman JB, Frisch AE (1996) Exploring chemistry with electronic structure methods, 2nd edn. Gaussian Inc., Pittsburgh, PA
9. Montgomery JA, Frisch MJ, Ochterski JW, Petersson GA (1999) *J Chem Phys* 110:2822–2827
10. Curtiss LA, Raghavachari K, Trucks GW, Pople JA (1991) *J Chem Phys* 94:7221–7230
11. Petersson GA, Bennet A, Tensfeldt TG, Al-Laham MA, Shirley WA, Mantzaris J (1988) *J Chem Phys* 89:2193–2218
12. Petersson GA, Al-Laham MA (1991) *J Chem Phys* 94:6081–6090
13. Adamo C, Barone V (1999) *J Chem Phys* 110:6158–6170
14. Perdew JP, Burke K, Ernzerhof M (1996) *Phys Rev Lett* 77:3865–3868
15. Flores-Holguin N, Glossman-Mitnik D (2004) *J Mol Struct Theochem* 681:77–82
16. Flores-Holguin N, Glossman-Mitnik D (2005) *J Mol Struct Theochem* 717:1–3
17. Flores-Holguin N, Glossman-Mitnik D (2005) *J Mol Struct Theochem* 723:231–234
18. Mendoza-Wilson AM, Glossman-Mitnik D (2004) *J Mol Struct Theochem* 681:71–76

19. Mendoza-Wilson AM, Glossman-Mitnik D (2005) *J Mol Struct Theochem* 716:67–72
20. Rodriguez-Valdez LM, Martinez-Villafane A, Glossman-Mitnik D (2005) *J Mol Struct Theochem* 681:83–88
21. Rodriguez-Valdez LM, Martinez-Villafane A, Glossman-Mitnik D (2005) *J Mol Struct Theochem* 716:61–65
22. Glossman-Mitnik D (2007) *Theor Chem Acc* 117:57–68
23. Glossman-Mitnik D (2007) *J Mol Model* 13:43–46
24. Lewars E (2003) Computational chemistry - introduction to the theory and applications of molecular and quantum mechanics. Kluwer, Norwell, MA, USA
25. Stratmann RE, Scuseria GE, Frisch MJ (1998) *J Chem Phys* 109:8218–8224
26. Bauernschmitt R, Ahlrichs R (1996) *Chem Phys Lett* 256:454–464
27. Casida ME, Jamorski C, Casida KC, Salahub DR (1998) *J Chem Phys* 108:4439–4449
28. Thompson MA, Zerner MC (1991) *J Am Chem Soc* 113:8210–8215
29. Zerner MC (1991) In: Lipkowitz KB, Boyd DB (eds) *Reviews in computational chemistry*, vol 2. VCH, New York, pp 313–366
30. Zerner MC, Correa de Mello P, Hohenberger M (1982) *Int J Quant Chem* 21:251–258
31. Hanson LK, Fajer J, Thompson MA, Zerner MC (1987) *J Am Chem Soc* 109:4728–4730
32. Anderson WP, Edwards WD, Zemer MC (1986) *Inorg Chem* 25:2728–2732
33. Gorelsky SI (2005) SWizard program, <http://www.sg-chem.net/>
34. Yang W, Mortier WJ (1986) *J Am Chem Soc* 108:5708–5711
35. Hirshfeld FL (1977) *Theor Chim Acta* 44(2):129–138
36. Jensen LH (1954) *J Am Chem Soc* 76:4663–4667
37. Silverstein RM, Webster FX (1998) Spectrometric identification of organic compounds, 6th edn. Wiley, New York
38. http://www.aist.go.jp/RIODB/SDBS/cgi-bin/cre_index.cgi
39. Savitskaya AV, Paschenko LA, Dobrotvorsky AE (1989) Farmatsiya (Moscow, Russian federation) 38(5):39–44
40. Parr RG, Yang W (1989) Density functional theory of atoms and molecules. Oxford University Press, New York
41. <http://redpoll.pharmacy.ualberta.ca/drugbank/>
42. Takaki Y, Sasada Y, Watanabe T (1960) *Acta Crystallogr* 13:693–702
43. Chis V, Pirnau A, Jurca T, Vasilescu M, Simon S, Cozar O, David L (2005) *Chem Phys* 316:153–163
44. <http://webbook.nist.gov>
45. Gadret M, Goursolle M, Leger JM, Colleter JC (1975) *Acta Crystallogr B* 31(5):1454–1462
46. Ovcharova G, Dimitrova D, Kuneva K (1982) Farmatsiya (Sofia, Bulgaria) 32(4):49–53
47. Angeloni I, Marzocchi MP, Smulevich G (1984) *J Raman Spectrosc* 15(2):90–96
48. Kolandaivel P, Praveena G, Selvarengan P (2005) *J Chem Sci* 117 (5):591–598